Reverse Mode of the Sarcoplasmic Reticulum Calcium Pump and Load-Dependent Cytosolic Calcium Decline in Voltage-Clamped Cardiac Ventricular Myocytes

Thomas R. Shannon, Kenneth S. Ginsburg, and Donald M. Bers
Department of Physiology, Loyola University Chicago, Maywood, Illinois 60153 USA

ABSTRACT We have characterized $[Ca]_i$ decline in voltage-clamped rabbit ventricular myocytes with progressive increases in sarcoplasmic reticulum (SR) calcium load. "Backflux" through the SR calcium pump is a critical feature which allows realistically small values for SR calcium leak fluxes to be used. Total cytosolic calcium was calculated from the latter part of $[Ca]_i$ decline using rate constants for cellular calcium buffers. Intra-SR calcium buffering characteristics were also deduced. We found that the net SR calcium pump flux and rate of $[Ca]_i$ decline decreased as the SR free [Ca] rose, with pump parameters held constant. We have therefore characterized for the first time in intact myocytes both forward and reverse SR calcium pump kinetics as well as intra-SR calcium buffering and SR calcium leak. We conclude that the reverse flux through the SR calcium pump is an important factor in comprehensive understanding of dynamic SR calcium fluxes.

INTRODUCTION

Typical cardiac calcium transients in myocytes decline to a resting free cytosolic [Ca] ($[Ca]_i$) of ~100 nM (Table 1). There are three major processes responsible for this decline: 1) Calcium efflux to the extracellular fluid through the sodium-calcium exchanger; 2) calcium uptake into the sarcoplasmic reticulum (SR) through the SR calcium pump; and 3) the passive calcium leak from the SR (Bers, 1991; Bassani et al., 1994; Bassani and Bers, 1995). Minor contributions may also be made by the sarcolemmal calcium pump, passive sarcolemmal calcium leak, and mitochondrial calcium uptake (Bassani et al., 1992, 1993; Trafford et al., 1998). The final $[Ca]_i$ depends upon the balance between these fluxes. We have concentrated upon the SR calcium pump and passive SR calcium leak in this work.

SR calcium pump transport has been described by the classic Hill equation balanced by a non-pump-mediated leak flux component (Klein et al., 1991; Sipido and Wier, 1991; Balke et al., 1994; Luo and Rudy, 1994a, b; Wier et al., 1994) e.g., the SR calcium release channel). This means that at rest when total SR calcium ($[Ca]_{SRT}$) is relatively constant, the SR calcium pump rate must be about the same as the leak. However, for a SR calcium pump K_m of 0.2–0.6 μM calcium the resting steady-state calcium leak flux would be ~⅕ of the pump V_{max}. Such a large pump flux would consume ATP at a relatively high rate in the resting myocyte, thus unnecessarily depleting the cell of energetic phosphate. Such a pump-leak balance would therefore be costly and inefficient.

A large pump-leak flux does not take place in the resting myocyte. It has been shown that the maximal $[Ca]_{SRT}$ is relatively independent of SR calcium pump velocity (Ginsburg et al., 1998). This indicates that the SR calcium leak rate must be very low. Furthermore, Bassani and Bers (1995) measured a unidirectional steady-state resting SR calcium leak flux in intact cells. Their value of 0.32 μM/s is more than 100 times slower than the pump-leak balance at resting $[Ca]_i$ referred to above. These measurements were also consistent with resting calcium spark data, which indicate that the SR calcium leak flux rate is between 0.2 and 0.8 μM/s (Cheng et al., 1993).

Accumulated free intra-SR [Ca] ($[Ca]_{SR}$) must therefore slow net SR calcium pump rate, nearly stopping it when resting $[Ca]_i$ has been achieved. $[Ca]_{SR}$ would cause a unidirectional flux of calcium from the SR to the cytosol mediated by the SR calcium pump (which we term "backflux"). In this model (Fig. 1), a thermodynamic SR calcium gradient builds as calcium is transported into the SR. The energy within this gradient is derived from the free energy available from cytosolic ATP (ΔG_{ATP}) which drives the pump in the forward mode. Backflux through the pump can produce ATP from ADP + P_i, which is the reversal of the reaction coupled with the forward pump flux. Indeed, this sort of backflux has been demonstrated in SR membrane vesicles (Weber et al., 1966; Makinose, 1971; Takenaka et al., 1982; Feher and Briggs, 1984) but it is not clear how this works in intact myocardial cells. The ATP production in the coupled backflux reaction would result in much less cellular energy use than the less efficient pump-leak balance.

We have developed a method to derive SR calcium uptake as a function of total cytosolic [Ca] ($[Ca]_T$; as $d[Ca]_T/dt$) at different $[Ca]_{SRT}$ in ventricular myocytes. $[Ca]_T$ was derived from $[Ca]_i$ by accounting for the major cytosolic calcium buffers. An equation was used which accounts for backflux to fit the data using realistic leak parameters. Values for all relevant parameters are given.

Received for publication 27 May 1999 and in final form 20 October 1999.
Address reprint requests to Dr. Donald M. Bers, Dept. of Physiology, Loyola University Medical Center, 2160 S. First Ave., Maywood, IL 60153-5505. Tel.: 708-216-1018; Fax: 708-216-6308; E-mail: dbers@luc.edu.

0006-3495/00/01/322/12 $2.00

TABLE 1 Abbreviations

Abbreviation	Definition
SR	Sarcoplasmic reticulum
$[Ca]_i$	Free cytosolic calcium
$[Ca]_T$	Total cytosolic calcium
$[Ca \cdot L]$	Bound cytosolic calcium
$[Ca]_{SR}$	Free SR calcium
$[Ca]_{SRT}$	Total SR calcium
I_{Ca}	L-type calcium current
J_{pumpf}	SR calcium pump forward mode flux
J_{pumpr}	SR calcium pump backflux
J_{leak}	SR calcium passive leak flux
J_{rel}	SR calcium release flux
Hf	Hill coefficient of the SR calcium pump forward mode
Hr	Hill coefficient of backflux
K_{mf}	K_m of the forward mode of the SR calcium pump
K_{mr}	K_m of the reverse mode of the SR calcium pump
V_{maxf}	V_{max} of the forward mode of the SR calcium pump
V_{maxr}	V_{max} of the reverse mode of the SR calcium pump
B_{max-SR}	B_{max} for calcium binding within the SR
K_{d-SR}	K_d for calcium binding within the SR
k	SR leak rate constant

MATERIALS AND METHODS

All chemicals were from Sigma Chemical Co. (St. Louis, MO), except as indicated. Voltage clamp data were collected and analyzed with PClamp (Axon Instruments, Foster City, CA). Further mathematical data manipulation was performed using Lotus 1-2-3 (Lotus Development Corp., Toronto, Ontario). Nonlinear regression fits were done with SigmaPlot and TableCurve (SPSS Software Products, San Rafael, CA), Origin (Microcal Software, Inc., North Hampton, MA) and GraphPad (iSi Software, Philadelphia, PA).

Cell preparation

Rabbit ventricular myocytes were isolated as described previously (Hryshko et al., 1989). Briefly, New Zealand White rabbits were anesthetized with sodium pentobarbital and their hearts were excised. Hearts were perfused with nominally calcium-free Tyrode's solution for 5 min followed by 20 min of perfusion with 1 mg/ml collagenase B (Boehringer Mannheim Corp., Indianapolis, Ind.) and 0.16 mg/ml protease (type X-IV, Sigma). After enzymatic digestion, the myocytes were filtered and washed twice in nominally calcium-free Tyrode's solution.

Experimental protocol

Voltage clamp protocol

SR calcium transport under different SR loading conditions was measured in voltage-clamped isolated ventricular myocytes. The SR was progressively loaded with I_{Ca} essentially as described by Ginsburg et al. (1998). I_{Ca} was recorded in the ruptured patch mode. Borosilicate glass electrodes of 1–2 MΩ were filled with 1 μM Ru360 and (in mM) 0.1 K_5-indo-1, 40 CsCl, 80 cesium-methanesulfonate, 0.5 $MgCl_2$, and 10 HEPES (pH 7.2). Ru360 inhibits mitochondrial calcium uptake (Matlib et al., 1998) and was the kind gift of Dr. M. A. Matlib, University of Cincinnati.

Cells were sodium-depleted by incubating for 5–30 min in sodium- and calcium-free solution containing (in mM) 140 LiCl, 6 KCl, 1 $MgCl_2$, 1 EGTA, 10 glucose, and 10 HEPES (pH 7.4). I_{Ca} was recorded in the absence of sodium-calcium exchange by perfusion with a sodium-free solution containing (in mM) 140 TEA-Cl, 2 $CaCl_2$, 4 CsCl, 1 $MgCl_2$, 10 glucose, and 10 HEPES (pH 7.4). There was therefore no sodium inside or outside the cell, eliminating sodium-calcium exchange fluxes in these experiments.

Fig. 2 illustrates the experimental protocol. Caffeine and sodium were applied to deplete the SR of calcium. The empty SR was progressively loaded in the absence of sodium via I_{Ca} with repeated 200-ms depolarizations from a holding potential of −55 to 0 mV at 0.25 Hz. The number of pulses was varied from between 1 and 20 to give different $[Ca]_{SRT}$. Subsequent caffeine application in sodium-free solution caused SR calcium release. Peak $[Ca]_i$ was used to measure $[Ca]_{SRT}$ (in the absence of efflux via the sodium-calcium exchanger). A caffeine-containing solution with 140 NaCl instead of TEA-Cl was introduced 2 s later to allow cellular calcium efflux and re-initialize the SR calcium load. Caffeine-free sodium-free solution were then restored. Integration of sodium-calcium exchange current under these conditions yielded similar $[Ca]_{SRT}$ to those when peak $[Ca]_i$ was used (Ginsburg et al., 1998).

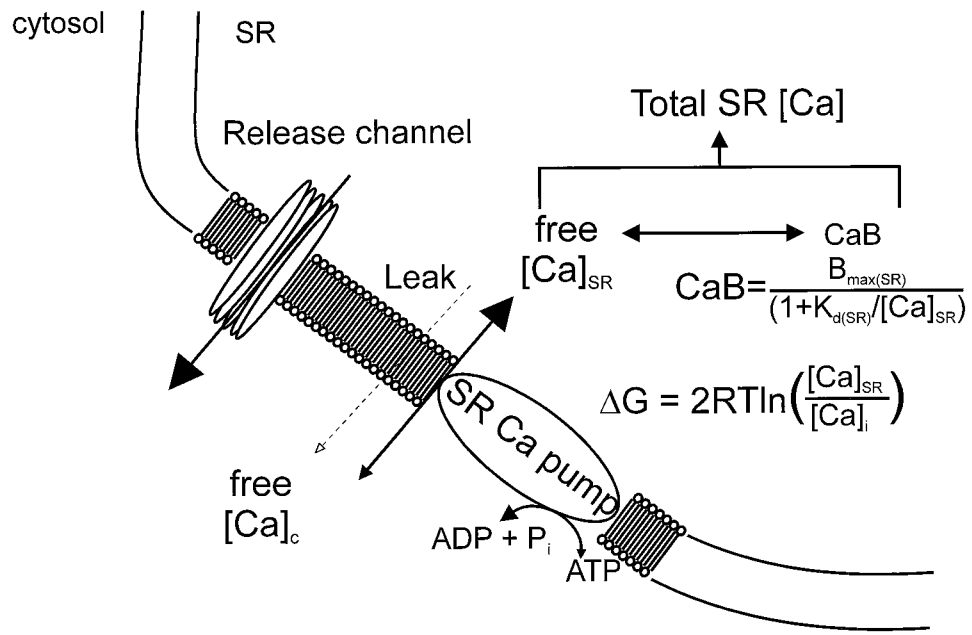

FIGURE 1 Model of the sarcoplasmic reticulum showing the relevant fluxes across the membrane. These include a passive leak, active forward, and reversal reverse modes of the SR calcium pump.

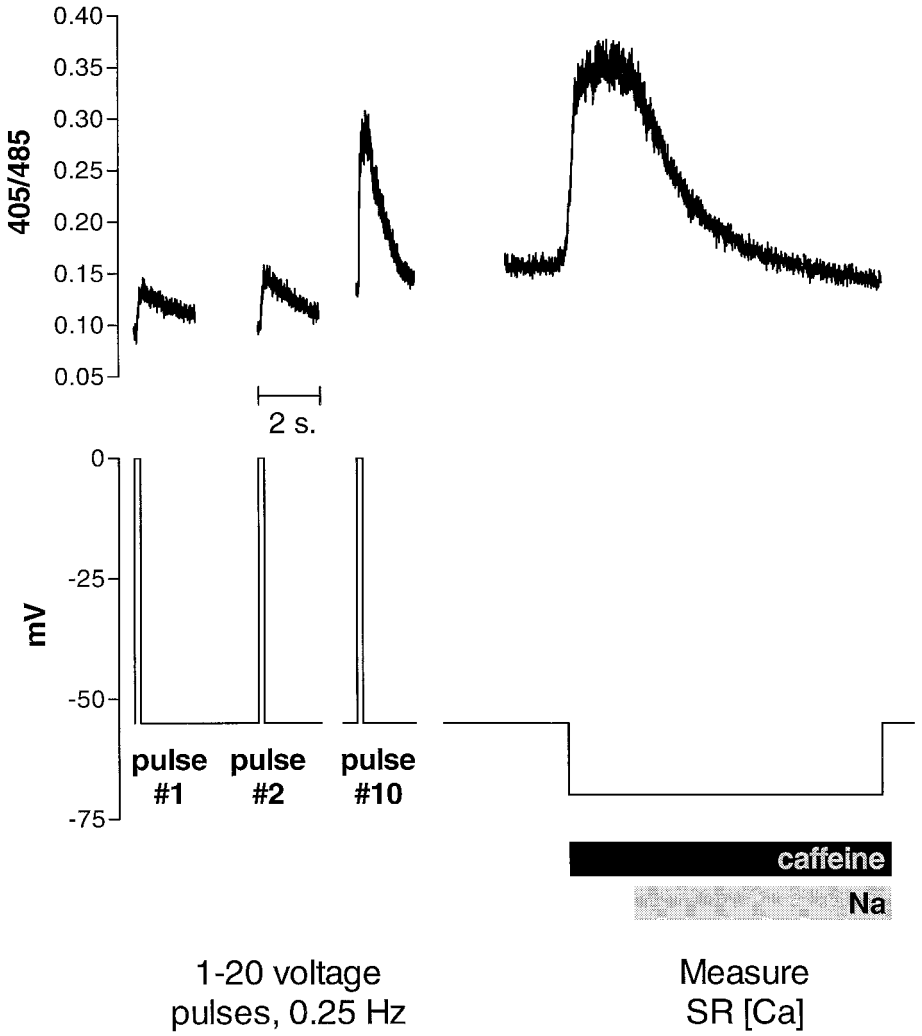

FIGURE 2 SR calcium uptake in intact Na_i-depleted rabbit ventricular myocytes under ruptured-patch voltage clamp, using sodium-free solutions to block $I_{Na/CaX}$. In each cell, the SR was first unloaded with caffeine, then calcium-loaded in a series of 1–20 voltage-clamp pulses to 0 mV via I_{Ca}. After each pulse train, the resulting $[Ca]_{SRT}$ was released with caffeine and deduced from the peak indo-1 fluorescence.

Fluorescence values at 405 and 485 (F_{405} and F_{485}) were background-subtracted and the ratio of the values (R) was converted to calcium bound to indo-1 ligand:

$$[\mathrm{Ca}\cdot indo] = \frac{[\mathrm{indo}]_T}{1 + (R_{max} - R)/\beta(R - R_{min})} \quad (1)$$

$[\mathrm{indo}]_T$ is the total indo in the cell. R_{min} and R_{max} were measured in vivo as previously described (Bassani et al., 1995a). The measured proportionality constant (β) was 3.0.

Measurement of indo-1 concentration

Calcium bound to indo-1 is dependent upon the amount of dye that has diffused from the pipette into the cytosol. In order to calculate this concentration, a $[Ca]_i$-independent variable, F_c, was measured (Zhou et al., 1998):

$$F_c = F_{405} + \alpha F_{485} \quad (2)$$

where α is the "isocoefficient," a constant that is the negative slope of the relationship between F_{485} and F_{405} during the twitch. This parameter is constant at different $[Ca]_i$ for a setup with fixed optical hardware. At time t, $[\mathrm{indo}]_T$ is directly proportional to F_c. Then $[\mathrm{indo}]_T = [\mathrm{indo}]_{pipette}F_c(t)/F_c(\infty)$ and $F_c(t) = F_c(\infty)(1 - \exp(-t/\tau))$, where τ is a function of series resistance and cell size (Zhou et al., 1998).

Determination of $[Ca]_i$

Rather than using the usual indo-1 transient directly to infer $[Ca]_i$, we corrected for the kinetics of the indicator. Using the $[Ca \cdot indo]$ from Eq. 1, $[Ca]_i$ was calculated after rearrangement of the general rate equation for each ligand (L) considered:

$$\frac{d[\mathrm{Ca}\cdot L]}{dt} = k_{on}([\mathrm{Ca}]_i)L - k_{off}([\mathrm{Ca}\cdot L]) \quad (3)$$

where calcium bound to ligand $[Ca \cdot L]$ is $[Ca \cdot indo]$, L equals ($[\mathrm{indo}]_T - [Ca \cdot indo]$), and k_{on} and k_{off} are the on and off rate constants for binding (Table 2). Note that instantaneous Ca-indo binding kinetics are not assumed. $[Ca]_i$ transients and calcium currents were empirically smoothed either using TableCurve (SPSS Software Products, Fig. 3) or with an equation of multiple exponential components. All of the calcium transients and calcium currents from all of the pulses in a given pulse protocol were smoothed and concatenated to determine true steady-state levels for all subsequently examined parameters.

TABLE 2 Intact myocyte cytosolic calcium buffering parameters

Buffer	B_{max} (μmol/l cytosol)	K_d (μM)	k_{off} (/s)	k_{on} (/μM · s)
Troponin C*†	70	0.6	19.6	32.7
Troponin C calcium/magnesium‡*	140	0.0135	0.032	2.37
(Mg sites)‡*		1111	3.33	0.003
SR calcium pump§	47	0.6	60	100
Calmodulin¶‖	24	7	238	34
Sarcolemma**	42	13	1300	100
Membrane/High††	15	0.3	30	100
Myosin calcium/magnesium*	140	0.0333	0.46	13.8
(Mg sites)*		3.64	0.057	0.0157
Indo-1§ ‡‡ ¶¶	<100	0.6	60	100

*Robertson et al., 1981.
†Gao et al., 1994.
‡Pan and Solaro, 1987.
§k_{off} calculated from K_d assuming k_{on} is diffusion-limited.
¶Haiech et al., 1981.
‖The four calcium-calmodulin binding sites were lumped as a single site. The K_d was artificially increased so that the steady-state calcium-calmodulin binding was well predicted over the relevant range of $[Ca]_i$ (0.1–3 μM) without requiring separate kinetic calculations of magnesium and potassium competition at each of the four sites.
**Post and Langer, 1992.
††Bers et al., 1986.
‡‡Jackson et al., 1987.
¶¶Indo-1 concentration was determined as described in Methods.

Calculation of cellular calcium fluxes

Our aim in this paper and the following companion paper (Shannon et al., 2000) was to determine the SR calcium fluxes (J_{SR}). These were determined as a function of the global cytosolic calcium flux ($d[Ca]_T/dt$) where:

$$\frac{d[Ca]_T}{dt} = \frac{d[Ca]_i}{dt} + \frac{d[Ca \cdot L]_T}{dt} + J_{SR} + J_{NaCaX} + J_{I_{Ca}} + J_{mito} + J_{SLpump} \quad (4)$$

and therefore

$$J_{SR} = \frac{d[Ca]_T}{dt} - \left(\frac{d[Ca]_i}{dt} + \frac{d[Ca \cdot L]_T}{dt} + J_{NaCaX} + J_{I_{Ca}} + J_{mito} + J_{SLpump}\right) \quad (5)$$

$J_{I_{Ca}}$ is the calcium current flux that was converted to μM/s using a capacitance/volume ratio of 6.44 pF/pL cytosol (Satoh et al., 1996). The sodium-calcium exchange flux (J_{NaCaX}) across the SL membrane is zero with sodium-free conditions. The mitochondrial calcium flux (J_{mito}) is assumed to be zero in our experiments since Ru360 is present. The sarcolemmal calcium pump flux (J_{SLpump}) has been estimated to be 37 times slower than the SR calcium pump flux (Bassani et al., 1992) and assumed to be negligible in these experiments. This leaves only $d[Ca]_T/dt$ and the rate of calcium binding to cytosolic buffers ($d[Ca \cdot L]_T/dt$) to be determined.

Cytosolic calcium buffering

$[Ca]_T$ was calculated from $[Ca]_i$ using the calcium binding properties of known cellular calcium buffers (both endogenous and added, Table 2). Because the rise and fall of calcium during the transient is relatively rapid, we did not assume instantaneous binding kinetics for any of the buffers during the $[Ca]_i$ transient. Total calcium binding change was calculated using Eq. 3 for each of the eight ligands (L) in Table 2 and:

$$\frac{d[Ca \cdot L]_T}{dt} = \sum_{j=1}^{8} \frac{d[Ca \cdot L]_j}{dt} \quad (6)$$

$d[Ca \cdot L]_T/dt$ was numerically integrated from time $t = 0$ to n:

$$[Ca \cdot L]_T = ([Ca \cdot L]_T)_{t=0} + \int_{t=0}^{n} \frac{d[Ca \cdot L]_T}{dt} \quad (7)$$

SR calcium fluxes

All fluxes on the right side in Eq. 5 are now accounted for and J_{SR} can be calculated from the $[Ca]_i$ transients and I_{Ca}. The components of J_{SR} were determined:

$$J_{SR} = J_{pump} + J_{rel} + J_{leak} \quad (8)$$

where J_{pump} is the net pump flux of the SR calcium pump and J_{leak} is the passive leak flux. J_{rel} is the release flux of calcium through the SR calcium release channel. J_{rel} was zero in these experiments because only the late part of the $[Ca]_i$ transient was used to measure J_{SR} in our experiments (i.e., the portion after SR release is over). J_{rel} will be considered in more detail in the following companion paper (Shannon et al., 2000).

SR calcium buffering

Equations describing net flux into a calcium-loaded SR will depend upon $[Ca]_{SR}$, which is not a directly measured variable. $[Ca]_{SR}$ can, however, be

calculated from the following relationship:

$$[Ca]_{SRT} = [Ca \cdot L]_{SR} + [Ca]_{SR} \quad (9)$$

$$[Ca]_{SRT} = \frac{B_{max-SR}([Ca]_{SR})}{K_{d-SR} + [Ca]_{SR}} + [Ca]_{SR} \quad (10)$$

where K_{d-SR} is the dissociation constant of SR proteins for calcium. This was set to 0.630 mM SR, previously determined using permeabilized myocyte and fractionated membrane preparations (Shannon and Bers, 1997) and similar to in vitro measures of calsequestrin binding (Mitchell et al., 1988; Slupsky et al., 1987). Note that instantaneous binding kinetics are assumed as suggested by the results of Donoso et al. (1995) for calsequestrin. These investigators found complete dissociation of calcium from calsequestrin in <1 ms (the resolution of their stopped-flow measurement). $[Ca]_{SRT}$ at the end of the last $[Ca]_i$ transient (time $t = n$) in a series is measured with caffeine. At this point $[Ca]_{SRT}$ at the beginning of the transient ($t = 0$) can be back-calculated. Total cell calcium (i.e., $[Ca]_{SRT} + [Ca]_T$) at $t = n$ equals total calcium at $t = 0$ plus all of the calcium that enters during the transient (i.e., I_{Ca}). Therefore:

$$([Ca]_{SRT})_{t=0} = (([Ca]_{SRT})_{t=n} + ([Ca]_T)_{t=n}) - \left(([Ca]_T)_{t=0} + \int_{t=0}^{n} I_{Ca}dt\right) \quad (11)$$

$[Ca]_{SRT}$ was then incremented with time:

$$\Delta[Ca]_{SRT} = \int I_{Ca}dt - \Delta[Ca]_T \quad (12)$$

Equation 10 was solved for $[Ca]_{SR}$ and substituted into all of the equations below. Therefore B_{max-SR} was an additional free parameter in these equations.

Values for $[Ca]_T$ were converted from units of μmol/l cytosol to μM SR by assuming the SR volume is 3.5% of the total cell volume and that 65% of the cell volume is cytosol (Page et al., 1971; Page, 1978). The final conversion factor was 18 l cytosol/l SR.

SR calcium uptake and leak

For the purpose of comparison, calcium uptake data were fit with two separate equations. The first was the standard Hill equation:

$$J_{pump} = \frac{V_{max}}{1 + (K_m/[Ca]_i)H} \quad (13)$$

where V_{max} is the maximum velocity of uptake, H is the Hill coefficient and K_m is the $[Ca]_i$ at which J_{pump} is at half of V_{max}. Note that there are no parameters to account for $[Ca]_{SRT}$ within the Hill equation.

SR calcium uptake data were also fit to a second equation which accounts for backflux as well as leak.

$$J_{SR} = \frac{V_{maxf}\left(\frac{[Ca]_i}{K_{mf}}\right)^{Hf} - V_{maxr}\left(\frac{[Ca]_{SR}}{K_{mr}}\right)^{Hr}}{1 + \left(\frac{[Ca]_i}{K_{mf}}\right)^{Hf} + \left(\frac{[Ca]_{SR}}{K_{mr}}\right)^{Hr}} + k([Ca]_{SR} - [Ca]_i) \quad (14)$$

where V_{maxf}, K_{mf}, and Hf are the usual Hill parameters for the forward pump flux and V_{maxr}, K_{mr}, and Hr are the same parameters for backflux. The leak portion of the equation ($J_{leak} = k \cdot \Delta[Ca]$) is a rearrangement of Fick's First Law where the molar flux density becomes the leak flux (J_{leak}) when the permeability in volume units becomes a simple rate constant (k). K_m was set to 260 nM (Hove-Madsen and Bers, 1993b; Bassani et al., 1994; Balke et al., 1994). k was constrained such that the leak was 0.32 μM/s at 106 μM/l cytosol $[Ca]_{SRT}$ and 0.1 μM $[Ca]_i$ (Bassani and Bers, 1995). Note that when $[Ca]_{SR} = 0$, the first (i.e., non-leak) portion of Eq. 14 reduces to Eq. 13.

Fits to Eq. 14 were constrained as indicated in Table 3. Among these was constraint according to the Haldane relationship ($K_{eq} = K_{mr}/K_{mf}$) where the SR calcium pump equilibrium constant (K_{eq}) is related to the free energy stored in the SR calcium gradient when the pump is at steady state (ΔG_{SRCa}):

$$\Delta G_{SRCa} = 2RT \ln K_{eq} = 2RT \ln \frac{[Ca]_{SR}}{[Ca]_i} \quad (15)$$

Therefore K_{eq} is the steady-state SR calcium gradient. This gradient of 7000 has been determined (Shannon and Bers, 1997) and was used here.

Individual I_{Ca} pulses and $[Ca]_i$ transients were fit to Eq. 14. Fixed parameters were K_{mf} (260 nM) and K_{d-SR} (0.63 mM SR). Several other parameters were explicitly constrained: $K_{mr} = 7000 \cdot K_{mf}$ (as above), $V_{maxr} = V_{maxf}$ (based upon the data of Takenaka et al., 1982), Hf = Hr (assuming the same stoichiometry in both directions), and k depends implicitly on B_{max-SR}. From Eq. 14 the leak rate constant can be defined as:

$$k = \frac{J_{leak}}{[Ca]_{SR} - [Ca]_i} \quad (16)$$

where $[Ca]_{SR}$ is an explicit quadratic function of $[Ca]_{SRT}$, B_{max-SR}, and K_{d-SR} by rearrangement of Eq. 10. Then, for $J_{leak} = 0.32$ μM/s, $[Ca]_i = 100$ nM, $[Ca]_{SRT} = 106$ μmol/l cytosol, and $K_{d-SR} = 0.630$ mM, B_{max-SR} and k are explicitly interdependent (i.e., fitting one fits both).

Thus there are only three free parameters (V_{maxf}, Hf, and B_{max-SR}) that are adjustable to simultaneously fit a series of calcium transients for both the $[Ca]_i$- and $[Ca]_{SR}$-dependence of net J_{SR}. The three free parameters were also limited to realistic values (see Table 3) and fits that fell to an extreme value of B_{max-SR} or V_{maxf} were discarded as inadequate to determine unique quantitative results regarding the SR calcium transport process.

TABLE 3 Best-fit parameters for SR calcium uptake in patch-clamped myocytes

Parameter	Mean ± SE	Comments/Constraints
V_{maxf}	137 ± 16 μM/s	Fit: limited $300 > V_{maxf} > 0$
V_{maxr}	137 ± 16 μM/s	Constrained: $V_{maxr} = V_{maxf}$
K_{mf}	260 nM	Fixed*
K_{mr}	1.8 mM	Fixed: $K_{mr} = 7000 \cdot K_{mf}$†
Hf	0.75 ± 0.10	Fit: limited $4 >$ Hf > 0.5
Hr	0.75 ± 0.10	Constrained: Hr = Hf
k	0.00047 ± 0.00004/s	Constrained: explicit f (B_{max-SR})‡
B_{max-SR}	2.7 ± 0.2 mM SR 140 μmol/l cytosol	Fit: $B_{max-SR} <225$ μmol/l cytosol,
K_{d-SR}	0.630 mM SR	Fixed†

$n = 19$ pulses in five cells. When a subset of cells that did not rise or fall to the maximum or minimum constraints on the Hill coefficient is considered, $V_{maxf} = V_{maxr} = 126 \pm 30$ μmol/l cytosol/s; Hf = Hr = 1.42 ± 0.42; $B_{max-SR} = 113 \pm 22$ μmol/l cytosol/s; k = 0.00037 ± 0.0006/s ($n = 7$ in five cells).

*Hove-Madsen and Bers, 1993b; Balke et al., 1994; Bassani et al., 1994.

†Shannon and Bers, 1997.

‡Bassani and Bers, 1995; see text.

The net SR calcium pump flux was further broken down into forward and reverse fluxes:

$$J_{pumpf} = \frac{V_{maxf}\left(\frac{[Ca]_i}{K_{mf}}\right)^{Hf}}{1 + \left(\frac{[Ca]_i}{K_{mf}}\right)^{Hf} + \left(\frac{[Ca]_{SR}}{K_{mr}}\right)^{Hr}} \quad (17)$$

$$J_{pumpr} = \frac{V_{maxr}\left(\frac{[Ca]_{SR}}{K_{mr}}\right)^{Hr}}{1 + \left(\frac{[Ca]_i}{K_{mf}}\right)^{Hf} + \left(\frac{[Ca]_{SR}}{K_{mr}}\right)^{Hr}} \quad (18)$$

RESULTS

Figure 3 shows four calcium transients (*B*) from one series of I_{Ca} pulses and their associated calcium currents (*A*) at different loads. The higher pulses are those in which more calcium has progressively accumulated within the SR. The calcium transients as well as the calcium currents were smoothed in order to minimize noise, which complicates the analysis. All of the calcium transients and calcium currents in the following figures are data that have been collected, then smoothed in this manner. They are not simulations.

Diastolic calcium rose gradually with the number of pulses in 0 Na solution (Figs. 2 and 3 *B*). This is likely due to the increased $[Ca]_{SRT}$ at steady state as demonstrated in Fig. 4 *A*. In this figure $[Ca]_{SRT}$ is shown as a function of the number of pulses under 0 Na conditions. $[Ca]_{SRT}$ rises with the number of pulses to a near maximum that is limited by the $[Ca]_{SR}$ (Ginsburg et al., 1998). With this result in mind $d[Ca]_i/dt$ was measured at 250 nM $[Ca]_i$ for calcium transients that rose to peaks above that level. These are plotted as a function of $[Ca]_{SRT}$ in Fig. 4 *B*. $d[Ca]_i/dt$ clearly slows as the SR calcium content rises (at a given $[Ca]_i$). We conclude, therefore, that the voltage clamp protocol increases $[Ca]_{SRT}$ to levels that alter $[Ca]_i$ decline. However, this simple analysis of essentially raw data is not sufficient for quantitative understanding of how backflux via the SR calcium pump slows net J_{SR}. This requires more detailed analysis of the calcium transient.

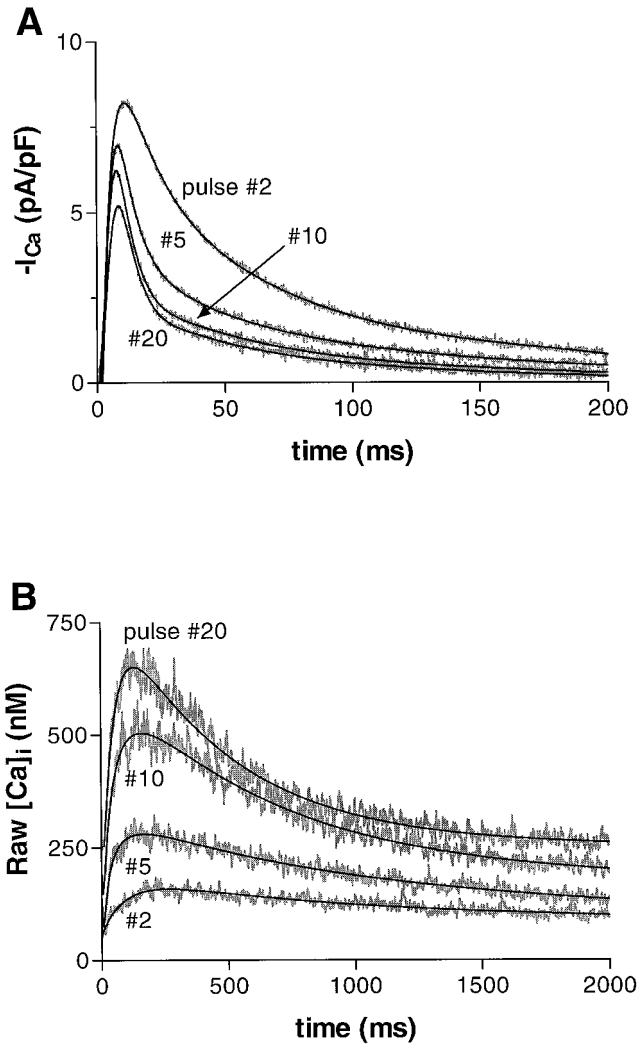

FIGURE 3 Typical calcium currents (*A*) and raw cytosolic free calcium transients (*B*) after repeated voltage-clamp pulses (*gray*). Data were smoothed either with Table Curve (SPSS Software) or empirically by fitting to an equation containing a series of exponential association and dissociation components. $[Ca]_i$ rises with successive pulses as SR calcium accumulates with a constant ΔG_{ATP}.

Cytosolic calcium buffering

We used rate-dependent binding constants to calculate cytosolic buffering in patch clamped isolated intact myocytes because the rise and fall of calcium within the cytosol is relatively fast. Rate dependent on and off rate constants for known cytosolic calcium buffers were collected from the literature or deduced (Table 2). Where data for the on rate was unavailable, this parameter was assumed to be diffusion-limited ($100/(\mu M \cdot s)$).

Fig. 5 *B* shows the change in calcium bound to each of the cytosolic calcium buffers during the 10th calcium transient of a 10-pulse protocol (Fig. 5 *A*). The peak $[Ca]_T$ was typically $\approx$200 μmol/l cytosol under the conditions where the most calcium release was measured ($\Delta[Ca]_T \approx 75$ μmol/l cytosol).

Troponin C, the SR, and the sarcolemma bind the majority of the released calcium from the SR. The single buffer having the most bound calcium during the transient is the calcium/magnesium binding site of troponin C (>100 μmol/l cytosol) but the amount does not change much during the pulse. Binding to troponin C calcium/magnesium sites as well as to myosin comes down only slowly. Because of this slow dissociation, binding to these two buffers may not come back down to baseline in the 4 s between pulses (Robertson et al., 1981) as noted previously for parvalbumin

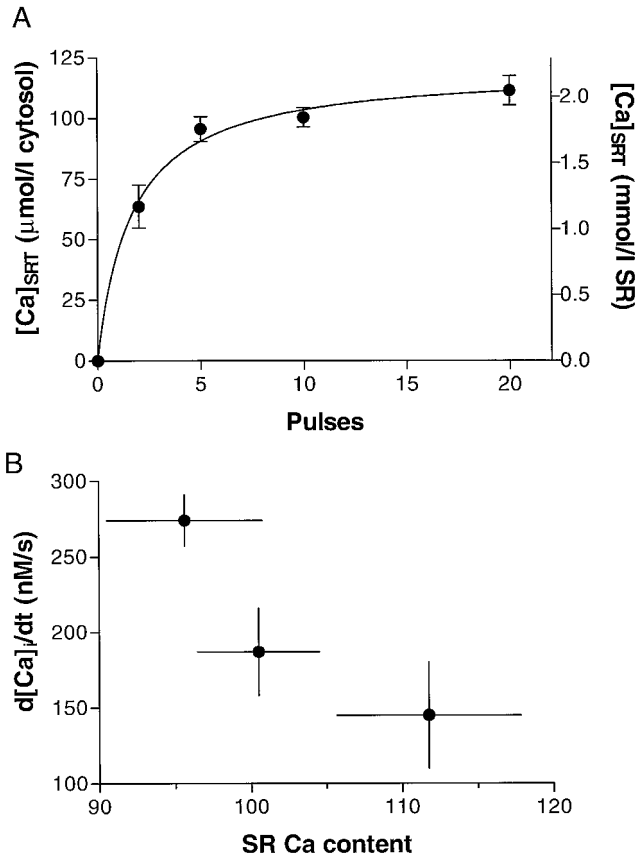

FIGURE 4 (*A*) SR calcium content after the execution of the voltage clamp protocol described in Fig. 2. $[Ca]_{SRT}$ rises with the number of pulses in 0 Na solution. (2 pulses, $n = 5$; 5 pulses, $n = 7$; 10 pulses, $n = 15$; 20 pulses, $n = 6$). (*B*) The decline in $[Ca]_i$ with increasing SR calcium load. $d[Ca]_i/dt$ was determined at 250 nM $[Ca]_i$ for all transients that reached this level (5 pulses, $n = 3$; 10 pulses, $n = 14$; 20 pulses, $n = 5$). The SR calcium contents were taken from *A*.

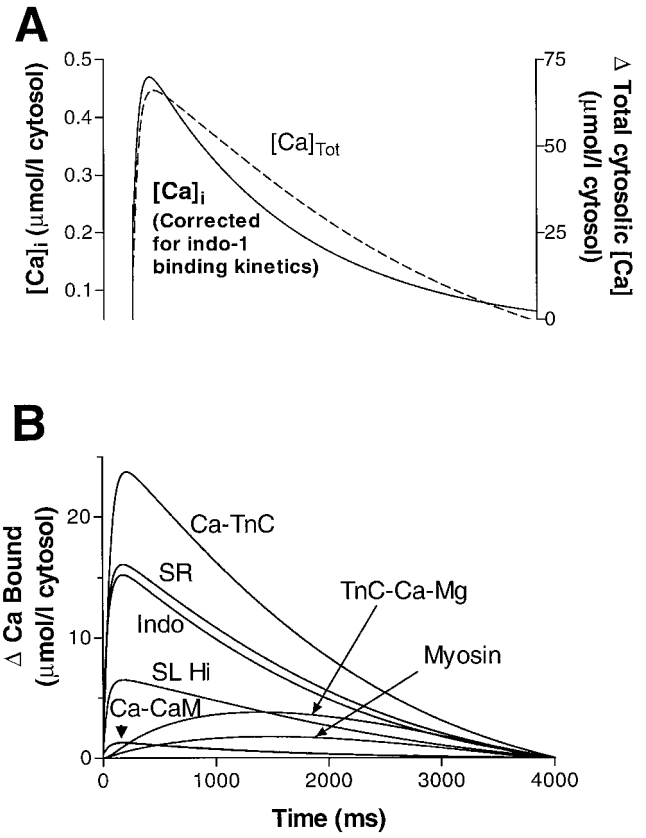

FIGURE 5 (*A*) $[Ca]_i$ (*solid line*) during a typical cellular steady-state calcium transient. The dashed line is the change in total cytosolic [Ca] during the transient after accounting for the cytosolic calcium buffers. (*B*) Calcium bound to individual cytosolic calcium buffers during the transient in *A*. The binding to these buffers was summed to give total cytosolic calcium.

in skeletal muscle and neural tissue (Baylor and Hollingworth, 1998; Yamada, 1999). Calcium binding to the calcium/magnesium sites on troponin C and to myosin therefore "ratchets up" from beat to beat until a steady state is reached after ≈5 pulses. This is shown in the smoothed $[Ca]_i$ transients (*A*) and corresponding troponin C calcium/magnesium binding (*B*) in Fig. 6.

SR calcium uptake

SR calcium uptake rate was calculated from $[Ca]_T$ as described in Methods. Data were converted to $[Ca]_T$ and J_{SR} was taken as the derivative of $[Ca]_T$ decline. Only the late part of the $[Ca]_i$ transient was used (after ≈300 ms) to be sure that J_{rel} was completed. The two panels of Figure 7 show the SR calcium uptake rate (*y* axis) from the same pulses as a function of $[Ca]_i$ (*A*) and $[Ca]_{SRT}$ (*B*). Note that as calcium is taken up from the cytosol and as $[Ca]_i$ declines (Fig. 7 *A*), $[Ca]_{SRT}$ (and $[Ca]_{SR}$) increase (Fig. 7 *B*). Both of these simultaneously result in a decline in SR calcium uptake rate. Shown in Fig. 7 are the uptake data from the last $[Ca]_i$ decline in a 10-pulse set and a 20-pulse set in the same cell. The decline of the 20th calcium transient in the 20-pulse set is against a higher $[Ca]_{SRT}$ than the decline from the 10th pulse in the 10-pulse set. Remember that sodium/calcium exchange is absent and calcium entry via I_{Ca} increases $[Ca]_{SRT}$. Also note that it takes a higher $[Ca]_i$ to achieve the same SR calcium uptake rate in Fig. 7 *A* when $[Ca]_{SR}$ is higher. This result is consistent with those in Fig. 4 *B*, where $d[Ca]_i/dt$ slows with increasing $[Ca]_{SRT}$ at the same $[Ca]_i$.

Any single SR calcium uptake could be fit well with the classic Hill equation (Eq. 13). For instance, the fit to the data from the decline of the 10th pulse in a 10-pulse protocol is shown in Fig. 7 *A*. However, it is apparent that uptakes from pulses at higher SR [Ca] deviate dramatically from this curve. At least part of the reason for this is because uptake at each $[Ca]_i$ is slowed with the increased $[Ca]_{SRT}$ in these pulses (Fig. 7 *B*). The deviation is not surprising since the Hill equation contains no mathematical terms that ac-

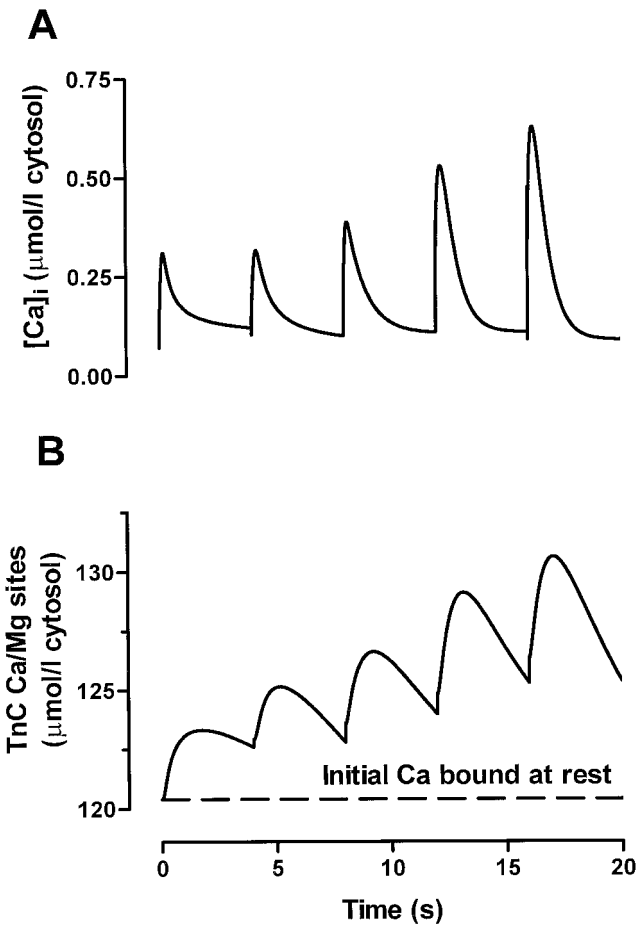

FIGURE 6 (*A*) Smoothed and kinetically corrected $[Ca]_i$ from five successive I_{Ca} pulses and calcium binding to troponin C calcium/magnesium binding site during the $[Ca]_i$ transients above. The binding to slow buffers "ratchets up" during successive pulses until a steady state is reached.

count for the increase in $[Ca]_{SR}$. Instead, such pulses at higher $[Ca]_{SRT}$ need to be fit individually with Hill equations having progressively higher K_m values (and altered Hill coefficients) at higher $[Ca]_{SRT}$. There is no a priori reason to think that the characteristic K_m for the SR calcium ATPase increases in our experiments. Indeed, even if either cAMP- (or calcium/calmodulin-) dependent protein kinase were to be more activated, the K_m might decrease rather than increase. Moreover, since we know that the SR calcium ATPase can produce both forward and reverse flux, we explored whether constant (and interrelated) K_{mf} and K_{mr} could explain our results.

Analysis was also performed using Eq. 14, which that accounts for pump-mediated flux in both the forward and reverse directions plus a realistic passive leak component. In this case both the $[Ca]_i$-dependence and $[Ca]_{SRT}$-dependence are fit simultaneously (a three-dimensional curve fit). Individual pulses fit to Eq. 14 were used to determine the uptake parameters in a quantitative manner (Fig. 7 and Table 3). We found that the uptake parameters did not vary with pulse number or $[Ca]_{SRT}$. Indeed, multiple pulse sets could be simultaneously fit as $f([Ca]_i, [Ca]_{SRT})$ by a single set of the three adjustable parameters. This is remarkable considering 1) the difficulty fitting multiple sets of data under different loading conditions, and 2) the constraints placed upon the fit parameters. Data from all single pulses whose fits did not fall or rise to maximum or minimum constraints on V_{max} or B_{max-SR} were therefore pooled. A summary of the relevant derived parameters for SR calcium decline is in Table 3. SR buffering parameters for intact myocytes were found from the fits of the calcium decline as described above (with a K_{d-SR} of 630 μmol/l SR (Shannon and Bers, 1997). The B_{max-SR} was allowed to vary and was found to be 2.7 $\pm$ 0.2 mM SR (Table 3). V_{maxf} was found to be 137 $\pm$ 16 μM/s. We found that the fits were extremely sensitive to changes in Hf. That is, on a fit-by-fit basis, constraining Hf too harshly created especially poor fits. Therefore, unlike the other parameters, we included fits in Table 3 with Hill coefficients equal to maximum or minimum constraints. On average this had little effect upon B_{max-SR} and V_{max}, but lowered Hf (=Hr) from 1.42 to 0.75 (see Table 3 legend).

In order to test the sensitivity of the analysis to our choice of buffering constants, we tested the effect of reducing the SR calcium pump binding capacity to 50% of the value in Table 2. The SR calcium pump was chosen because it is among the endogenous buffers that bind the most calcium during the $[Ca]_i$ transient. In addition, the binding capacity could actually change during the transient depending upon the pump rate. Reducing the SR calcium pump B_{max} by 50% only reduced the V_{max} and K_m of the pump by 5% and the B_{max-SR} by 15%.

DISCUSSION

$[Ca]_i$ decline and SR calcium transport slow as $[Ca]_{SR}$ accumulates within cardiac myocytes and this is the primary reason why the decline levels off at resting $[Ca]_i$ (in the absence of sodium-calcium exchange). The SR pump must be considered a reversible thermodynamic enzymatic reaction where the forward rate depends on $[Ca]_i$ and the reverse rate on $[Ca]_{SR}$. The steady state for this system is where the energy required to establish the [Ca] gradient ($2RT \ln([Ca]_{SR}/[Ca]_i)$) is balanced by the free energy available from ATP (ΔG_{ATP}). In this context increasing $[Ca]_{SR}$ or [ADP] $[P_i]$ would shift this balance toward net SR calcium loss and synthesis of ATP. There is extensive evidence for such thermodynamic backflux via the SR calcium pump (Weber et al., 1966; Makinose, 1971; Takenaka et al., 1982; Feher and Briggs, 1984). Indeed, the reverse flux can be as fast as the forward flux (Takenaka et al., 1982).

Most previous studies have used only a forward pump rate (Eq. 13), which is balanced by a leak at steady state (Klein et al., 1991; Sipido and Wier, 1991; Balke et al., 1994; Luo and Rudy, 1994a, b; Wier et al., 1994). While

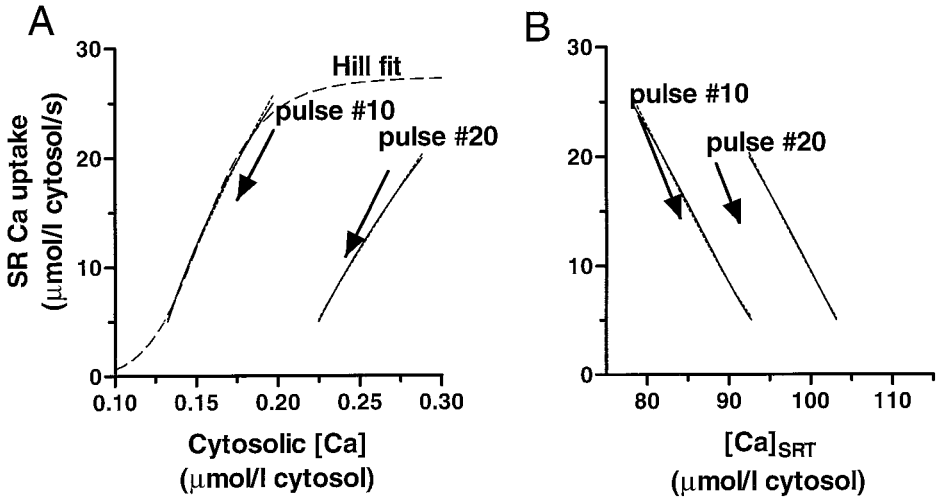

FIGURE 7 Uptake values as a function of $[Ca]_i$ (*A*) and of $[Ca]_{SRT}$ (*B*) are shown. Arrows indicate the time direction of the respective transient decline. The fit at lower $[Ca]_{SRT}$ is fit to the classical Hill equation (*long dashed line*). Both sets of data are fitted to the equation, which accounts for SR calcium pump reversibility (Eq. 14; *short dashed lines*). The data are much better described by this equation than by the Hill equation plus the leak function (not shown). Best-fit parameters are in Table 3.

this can satisfactorily describe calcium flux over a narrow range of conditions (Balke et al., 1994; Bassani et al., 1994), it is unrealistic to consider the net calcium pump rate to be independent of product concentration ($[Ca]_{SR}$). Furthermore, the amount of calcium leak required to balanced the forward pump rate is nearly 100 times higher than measured values for non-pump-mediated leak (Balke et al., 1994; Bassani et al., 1994; Bassani and Bers, 1995; 20 μM/s vs. 0.3 μM/s).

Cytosolic calcium buffering

It is important to note that the fundamental effect described in this report can be seen in the raw data. That is, $d[Ca]_i/dt$ declines for a given $[Ca]_i$ as the SR load rises (Fig. 4). Nevertheless, cytosolic calcium buffering characteristics are central to our analysis. Previously, calcium buffering has been measured directly in cells without resolving individual rate constants (Pierce et al., 1985; Hove-Madsen and Bers, 1993a; Berlin et al., 1994) or calculated based upon calcium binding properties of individual cellular constituents in more isolated systems (Fabiato, 1983; Balke et al., 1994).

We have used values that combine both approaches. That is, the sum of literature-based individual values behave as ensemble-like measurements of total cytosolic buffering in cardiac myocytes (Bers, 1999). These parameters (Table 2) include consideration of ligand binding kinetics and were defined at pH 7–7.2 and mostly at room temperature. Magnesium was assumed to be 0.5 mM, which is the concentration in the pipette and the approximate concentration within the intact cell (Blatter and McGuigan, 1986; Murphy et al., 1989a, b; Gao et al., 1994).

The $[Ca]_T$ peaks later than $[Ca]_i$ (Fig. 5 *A*). This is due to the fact that calcium influx and release are fast relative to the rate of binding to the majority of the cytosolic calcium buffers (Fig. 5 *B*). This is particularly true of troponin C calcium/magnesium binding sites (Fig. 6) and myosin. Binding to these two buffers is extremely slow, peaking late and falling only slowly. Because binding to these buffers does not come back to baseline after a single pulse, we conclude that steady-state level of binding to these buffers is dependent upon the interval between beats, and therefore stimulation rate. This can be demonstrated by accounting for the buffering during repeated voltage pulses using data from a given set of pulses (Fig. 6). After five voltage pulses, the level of binding to troponin C-calcium/magnesium rises from 121 to 126 μmol/l cytosol. If the stimulation rate is increased the levels of bound [Ca] are expected to rise to a higher steady-state level because binding after each pulse has even less time to decline.

SR calcium buffering

To include information about SR calcium pump backflux, knowledge of $[Ca]_{SR}$ is required. Free SR [Ca] is difficult to measure directly in the cardiac myocyte for at least two reasons: 1) the affinity of most available calcium-selective fluorescent dyes is too high to accurately measure $[Ca]_{SR}$ even at resting $[Ca]_i$ ($[Ca]_{SR}$ = 700 μmol/l SR), and 2) background fluorescence from mitochondria, which make up ~35% of the cellular volume, masks changes in fluorescence originating from a dye-loaded SR (Shannon and Bers, 1997).

Instead of direct measurement, we approached the problem of determining $[Ca]_{SR}$ by calculating it from $[Ca]_{SRT}$, which was measured by caffeine-induced transients. SR calcium buffering parameters from Shannon and Bers (1997) were used to do this. Given that the K_{d-SR} measured by Shannon and Bers (630 μmol/l SR) is very close to the K_d of calsequestrin measured in isolation (Mitchell et al., 1988; Slupsky et al., 1987), we used this K_{d-SR} and allowed the B_{max} to vary in our SR calcium flux fits. In this manner, we determined parameters for both SR calcium uptake and SR calcium buffering (Table 3, Figure 7).

Isolated myocytes, however, tend to demonstrate smaller $[Ca]_{SRT}$ than other systems (skinned fiber, papillary muscle, perfused heart, and permeabilized myocytes as reviewed in Bers, 1999). The reason for this is unknown but by allowing B_{max} to vary the data can be well described.

We have, therefore, for the first time estimated the SR calcium buffering characteristics of isolated intact ventricular myocytes. It is our hope that these buffering parameters may be useful to determine the effects of $[Ca]_{SR}$ on other cellular processes (Shannon et al., 2000).

The steady-state $[Ca]_i$ rises with increasing $[Ca]_{SRT}$ (Fig. 3 *B*). Although the steady-state $[Ca]_i$ is a balance of all of the fluxes across the SR membrane at rest, the primary reason for this rise is demonstrated by Eq. 15, which refers to the dominant SR calcium pump. The free energy (ΔG) stored within the [Ca] gradient across the SR membrane is dependent upon the ΔG_{ATP} within the cytosol (Shannon and Bers, 1997). This maximal calcium gradient is also dependent upon the degree of "slippage" or the uncoupling of calcium transport and ATP usage. Since ΔG_{ATP} is assumed to stay essentially constant during the time course of the experiments, ΔG_{SRCa} (and $[Ca]_{SR}/[Ca]_i$) would also stay constant at true steady state. Thus, diastolic $[Ca]_i$ and $[Ca]_{SR}$ tend to rise together in parallel. Each voltage pulse resulted in calcium uptake against a higher $[Ca]_{SRT}$ (Fig. 3 *B*). To the extent that $[Ca]_{SR}$ reaches a thermodynamic limit, this implies that doubling $[Ca]_{SR}$ would double $[Ca]_i$ (although $[Ca]_{SRT}$ would not increase proportionately as the buffers are saturable).

SR calcium pump fluxes in isolated myocytes

Backflux through the SR pump has been demonstrated in SR membrane vesicles (Weber et al., 1966; Makinose, 1971; Takenaka et al., 1982; Feher and Briggs, 1984) but its function in intact myocardial cells has not been appreciated. A key question is how big is the leak from the SR at rest. The SR calcium release channel is likely to be the highest source of leak from the SR. We used a leak rate that had been previously measured in normal intact cells in our laboratory with the SR calcium pump blocked in both forward and reverse modes by thapsigargin (Bassani and Bers, 1995). This is not to say that the leak rate is small under all conditions. For instance, SR calcium release channels under conditions of SR calcium overload may have a

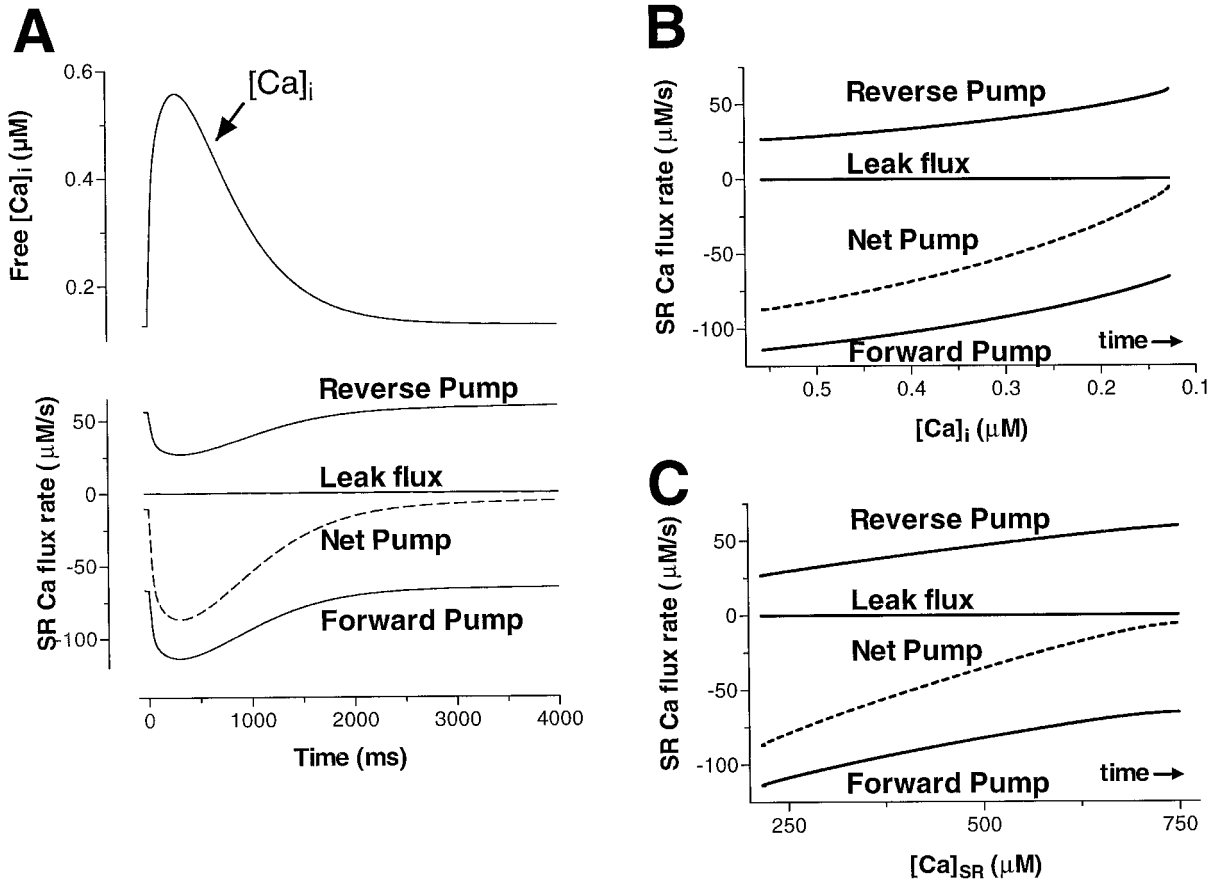

FIGURE 8 Unidirectional SR calcium fluxes as a function of time during the calcium transient (*A*) and as a function of $[Ca]_i$ (*B*) and $[Ca]_{SR}$ (*C*). SR calcium uptake rises as $[Ca]_i$ rises, then falls to a steady state where SR calcium uptake forward is equal to SR calcium pump reverse plus a small leak.

higher $[Ca]_i$ sensitivity (Bassani et al., 1995b; Spencer and Berlin, 1995, 1997; Santana et al., 1997; Dettbarn and Palade, 1997; Hüser et al., 1998). Such channels may have a higher open probability, resulting in higher leak. Theoretically, it should be possible to describe SR leak and SR calcium release with the same function. However, such an analysis would need to account for higher $[Ca]_i$ changes in a local cleft during ECC as opposed to rest, thus requiring additional assumptions.

The balance of SR pump fluxes and leak is demonstrated Fig. 8. Net SR calcium uptake rises as $[Ca]_i$ rises, then falls toward a value that at steady state will just counterbalance the leak (Fig. 8, *A* and *B*). Note that the reverse flux initially falls when $[Ca]_{SR}$ is low after SR calcium release. Then the reverse pump flux increases to almost offset forward pump flux. Therefore the reverse flux becomes a more and more significant component of the total net flux as $[Ca]_i$ declines to rest and $[Ca]_{SR}$ increases (Fig. 8, *A* and *C*). Note that at steady state $J_{pumpf} = J_{pumpr} + J_{leak}$. At 100 nM $[Ca]_i$ the SR calcium pump forward flux is equal to 33.8 μmol/(l cytosol · s). This is balanced by the flux out of the SR, which is the sum of the SR leak flux and the SR pump backflux. Note that J_{pumpr} (33.6 μmol/(l cytosol · s)) is almost equal to J_{pumpf}, while the J_{leak} is considerably smaller (0.2 μmol/(l cytosol · s)). This emphasizes the importance of the backflux reaction through the pump, since a leak rate of 33.8 μmol/(l cytosol · s) would be required in a pump leak balance, a value almost 20% of our V_{max}. Such a leak would use ≈150 times as much net ATP at rest to simply maintain a constant $[Ca]_{SRT}$. Since the reverse reaction of the pump produces ATP from ADP + P_i, ATP is relatively well conserved in a scheme that includes backflux.

In summary, we have described the decline in $[Ca]_i$ in myocardial cells in the absence of sodium/calcium exchange. This description included characterization of SR calcium uptake at different $[Ca]_{SRT}$. We conclude that the reversibility of the SR calcium pump should be accounted for when describing calcium dynamics within the cardiac cell.

The authors acknowledge the excellent technical assistance of Christina Zackavec, Steve Scaglione, and Sarah Wimbiscus.

This work was supported by National Institutes of Health Grants HL30077 and HL09412.

REFERENCES

Balke, C. W., T. M. Egan, and W. G. Wier. 1994. Processes that remove calcium from the cytoplasm during excitation-contraction coupling in intact rat heart cells. *J. Physiol.* 474:447–462.

Bassani, J. W. M., R. A. Bassani, and D. M. Bers. 1993. Ca^{2+} cycling between sarcoplasmic reticulum and mitochondria in rabbit cardiac myocytes. *J. Physiol.* 460:603–621.

Bassani, J. W. M., R. A. Bassani, and D. M. Bers. 1994. Relaxation in rabbit and rat cardiac cells: species-dependent differences in cellular mechanisms. *J. Physiol.* 476:279–293.

Bassani, J. W. M., R. A. Bassani, and D. M. Bers. 1995a. Calibration of indo-1 and resting intracellular $[Ca]_i$ in intact rabbit cardiac myocytes. *Biophys. J.* 68:1453–1460.

Bassani, J. W. M., W. Yuan, and D. M. Bers. 1995b. Fractional SR Ca release is regulated by trigger Ca and SR Ca content in cardiac myocytes. *Am. J. Physiol.* 268:C1313–C1329.

Bassani, R. A., J. W. M. Bassani, and D. M. Bers. 1992. Mitochondrial and sarcolemmal Ca^{2+} transport reduce $[Ca^{2+}]_i$ during caffeine contractures in rabbit cardiac myocytes. *J. Physiol.* 453:591–608.

Bassani, R. A., and D. M. Bers. 1995. Rate of diastolic Ca release from the sarcoplasmic reticulum of intact rabbit and rat ventricular myocytes. *Biophys. J.* 68:2015–2022.

Baylor, S. M., and S. Hollingworth. 1998. Model of sarcomeric Ca^{2+} movements, including ATP Ca^{2+} binding and diffusion, during activation of frog skeletal muscle. *J. Gen. Physiol.* 112:297–316.

Berlin, J. R., J. W. M. Bassani, and D. M. Bers. 1994. Intrinsic cytosolic calcium buffering properties of single rat cardiac myocytes. *Biophys. J.* 67:1775–1787.

Bers, D. M. 1991. Excitation-Contraction Coupling and Cardiac Contractile Force. Kluwer Academic Publishers, Dordrecht, The Netherlands.

Bers, D. M. 1999. Regulation of cellular Ca in cardiac myocytes. *In* Handbook of Physiology, edited by E. Page, H. A. Fozzard, R. J. Solaro. Oxford Press (in press).

Bers, D. M., L.-A. H. Allen, and Y.-J. Kim. 1986. Calcium binding to cardiac sarcolemmal vesicles: potential role as a modifier of contraction. *Am. J. Physiol.* 251:C861–C871.

Blatter, L. A., and J. A. S. McGuigan. 1986. Free intracellular magnesium concentration in ferret ventricular muscle measured with ion selective micro-electrodes. *Q. J. Exp. Physiol.* 71:467–473.

Cheng, H., W. J. Lederer, and M. B. Cannell. 1993. Calcium sparks: elementary events underlying excitation-contraction coupling in heart muscle. *Science.* 262:740–744.

Dettbarn, C., and P. Palade. 1997. Ca^{2+} feedback on "quantal" Ca^{2+} release involving ryanodine receptors. *Mol. Pharmacol.* 52:1124–1130.

Donoso, P., H. Prieto, and C. Hidalgo. 1995. Luminal calcium regulates calcium release in triads isolated from frog and rabbit skeletal muscle. *Biophys. J.* 68:507–515.

Fabiato, A. 1983. Calcium-induced release of calcium from the cardiac sarcoplasmic reticulum. *Am. J. Physiol.* 245:C1–C14.

Feher, J. J., and F. N. Briggs. 1984. Unidirectional calcium and nucleotide fluxes in sarcoplasmic reticulum. II. Experimental results. *Biophys. J.* 45:1135–1144.

Gao, W. D., P. H. Backx, M. Azan-Backx, and E. Marban. 1994. Myofilament Ca^{2+} sensitivity in intact versus skinned rat ventricular muscle. *Circ. Res.* 74:408–415.

Ginsburg, K. S., C. R. Weber, and D. M. Bers. 1998. Control of maximum sarcoplasmic reticulum Ca load in intact ferret ventricular myocytes: effects of thapsigargin and isoproterenol. *J. Gen. Physiol.* 111:491–504.

Haiech, J., B. Klee, and J. Demaille. 1981. Effects of cations on affinity of calmodulin for calcium: ordered binding of calcium ions allows specific activation of calmodulin-stimulated enzymes. *Biochemistry.* 20: 3890–3897.

Hove-Madsen, L., and D. M. Bers. 1993a. Passive Ca buffering and SR Ca uptake in permeabilized rabbit ventricular myocytes. *Am. J. Physiol.* 264:C677–C686.

Hove-Madsen, L., and D. M. Bers. 1993b. Sarcoplasmic reticulum Ca^{2+} uptake and thapsigargin sensitivity in permeabilized rabbit and rat ventricular myocytes. *Circ. Res.* 73:820–828.

Hryshko, L. V., V. M. Stiffel, and D. M. Bers. 1989. Rapid cooling contractures as an index of sarcoplasmic reticulum calcium content in rabbit ventricular myocytes. *Am. J. Physiol.* 257:H1369–H1377.

Hüser, J., D. M. Bers, and L. A. Blatter. 1998. Subcellular properties of $[Ca^{2+}]_i$-transients in phospholamban-deficient mouse ventricular cells. *Am. J. Physiol.* 274:H1800–H1811.

Jackson, A., M. Timmerman, C. Bagshaw, and C. Ashley. 1987. The kinetics of calcium binding to fura-2 and indo-1. *FEBS Lett.* 216:35–39.

Klein, M. G., L. Kovacs, B. J. Simon, and M. F. Schneider. 1991. Decline of myoplasmic Ca^{2+}, recovery of calcium release and sarcoplasmic Ca^{2+} pump properties in frog skeletal muscle. *J. Physiol.* 414:639–671.

Luo, C.-H., and Y. Rudy. 1994a. A dynamic model of the cardiac ventricular action potential. I. Simulations of ionic currents and concentration changes. *Circ. Res.* 74:1071–1096.

Luo, C.-H., and Y. Rudy. 1994b. A dynamic model of the cardiac ventricular action potential. II. After depolarizations, triggered activity, and potentiation. *Circ. Res.* 74:1097–1113.

Makinose, M. 1971. Calcium efflux dependent formation of ATP from ADP and orthophosphate by the membranes of the sarcoplasmic vesicles. *FEBS Lett.* 12:269–270.

Matlib, M. A., Z. Zhou, S. Knight, S. Ahmed, K. M. Choi, J. Krause-Bauer, R. Phillips, R. Altschuld, Y. Katsube, N. Sperelakis, and D. M. Bers. 1998. Oxygen-bridged dinuclear ruthenium amine complex specifically inhibits Ca^{2+} uptake into mitochondria in vitro and in situ in single cardiac myocytes. *J. Biol. Chem.* 273:10223–10231.

Mitchell, R. D., H. K. B. Simmerman, and L. R. Jones. 1988. Ca^{2+} binding effects on protein conformation and protein interactions of canine cardiac calsequestrin. *J. Biol. Chem.* 263:1376–1381.

Murphy, E., C. C. Freudenuich, L. A. Levi, U. E. London, and M. Lieberman. 1989a. Monitoring cytosolic free magnesium in cultured chicken heart cells by use of the fluorescent indicator furaptra. *Proc. Natl. Acad. Sci. USA.* 86:2981–2984.

Murphy, E., C. Steenbergen, L. A. Levy, B. Raju, and R. E. London. 1989b. Cytosolic free magnesium levels in ischemic rat heart. *J. Biol. Chem.* 264:5622–5627.

Page, E. 1978. Quantitative ultrastructural analysis in cardiac membrane physiology. *Am. J. Physiol.* 235:C147–C158.

Page, E., L. P. Mccallister, and B. Power. 1971. Stereological measurements of cardiac ultrastructures implicated in excitation-contraction coupling. *Proc. Natl. Acad. Sci. USA.* 68:1465–1466.

Pan, B. S., and J. Solaro. 1987. Calcium binding properties of troponin C in detergent-skinned heart muscle fibers. *J. Biol. Chem.* 262:7839–7849.

Pierce, G., K. Philipson, and G. Langer. 1985. Passive calcium-buffering capacity of a rabbit ventricular homogenate preparation. *Am. J. Physiol.* 249:C248–C255.

Post, J. A., and G. A. Langer. 1992. Sarcolemmal calcium binding sites in heart. I. Molecular origins in "gas-dissected" sarcolemma. *J. Membr. Biol.* 129:49–57.

Robertson, S. P., J. D. Johnson, and J. D. Potter. 1981. The time course of Ca^{2+} exchange with calmodulin, troponin, parvalbumin, and myosin in response to transient increases in Ca^{2+}. *Biophys. J.* 34:559–569.

Santana, L. F., E. G. Kranias, and W. J. Lederer. 1997. Calcium sparks and excitation-contraction coupling in phospholamban-deficient mouse ventricular myocytes. *J. Physiol.* 503:21–29.

Satoh, H., L. M. D. Delbridge, L. A. Blatter, and D. M. Bers. 1996. Surface:volume relationship in cardiac myocytes studied with confocal microscopy and membrane capacitance measurements: species-dependence and developmental effects. *Biophys. J.* 70:1494–1504.

Shannon, T. R., and D. M. Bers. 1997. Assessment of intra-SR free [Ca] and buffering in rat heart. *Biophys. J.* 73:1524–1531.

Shannon, T. R., K. S. Ginsburg, and D. M. Bers. 2000. Potentiation of fractional sarcoplasmic reticulum calcium release by total and free intra-sarcoplasmic reticulum calcium concentration. *Biophys. J.* 78: 334–343.

Sipido, K. R., and W. G. Wier. 1991. Flux of Ca^{2+} across the sarcoplasmic reticulum of guinea-pig cardiac cells during excitation-contraction coupling. *J. Physiol.* 435:605–630.

Slupsky, J. R., M. Ohnishi, M. R. Carpenter, and R. A. F. Reithmeier. 1987. Characterization of cardiac calsequestrin. *Biochemistry.* 26: 6539–6544.

Spencer, C. I., and J. R. Berlin. 1995. Control of sarcoplasmic reticulum calcium release during calcium loading in isolated rat ventricular myocytes. *J. Physiol.* 488:267–279.

Spencer, C. I., and J. R. Berlin. 1997. Calcium-induced release of strontium ions from the sarcoplasmic reticulum of rat cardiac ventricular myocytes. *J. Physiol.* 504:565–578.

Takenaka, H., P. N. Adler, and A. M. Katz. 1982. Calcium fluxes across the membrane of sarcoplasmic reticulum vesicles. *J. Biol. Chem.* 257: 12649–12656.

Trafford, A. W., M. E. Díaz, and D. A. Eisner. 1998. Stimulation of Ca-induced Ca release only transiently increases the systolic Ca transient: measurement of Ca fluxes and s.r. Ca. *Cardiovasc. Res.* 37:710–717.

Weber, A., R. Herz, and I. Reis. 1966. Study of the kinetics of calcium transport by isolated fragmented sarcoplasmic reticulum. *Biochem. J.* 345:329–369.

Wier, W. G., T. M. Egan, J. R. López-López, and C. W. Balke. 1994. Local control of excitation-contraction coupling in rat heart cells. *J. Physiol.* 474:463–471.

Yamada, K. 1999. Thermodynamic analyses of calcium binding to troponin c, calmodulin and parvalbumins by using microcalorimetry. *Mol. Cell. Biochem.* 190:39–45.

Zhou, Z., M. A. Matlib, and D. M. Bers. 1998. Cytosolic and mitochondrial Ca^{2+} signals in mammalian patch clamped ventricular myocytes. *J. Physiol.* 507:379–403.